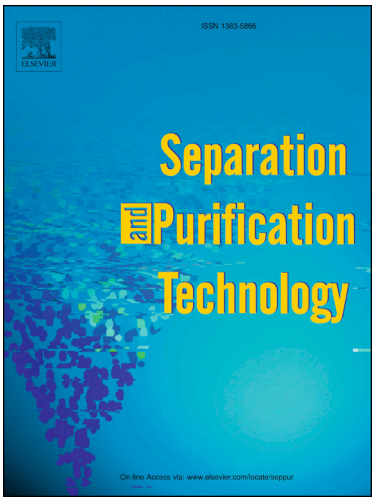

Selectively leaching the iron-removed bauxite residues with phosphoric acid for enrichment of rare earth elements

Bona Deng, Guanghui Li, Jun Luo, Qing Ye, Mingxia Liu, Mingjun Rao, Tao Jiang, Lukas Bauman, Boxin Zhao

PII: S1383-5866(19)30802-0
DOI: https://doi.org/10.1016/j.seppur.2019.115714
Article Number: 115714
Reference: SEPPUR 115714

To appear in: *Separation and Purification Technology*

Received Date: 27 February 2019
Revised Date: 8 May 2019
Accepted Date: 17 June 2019

Please cite this article as: B. Deng, G. Li, J. Luo, Q. Ye, M. Liu, M. Rao, T. Jiang, L. Bauman, B. Zhao, Selectively leaching the iron-removed bauxite residues with phosphoric acid for enrichment of rare earth elements, *Separation and Purification Technology* (2019), doi: https://doi.org/10.1016/j.seppur.2019.115714

An article submitted to *Separation and Purification Technology*

Selectively leaching the iron-removed bauxite residues with phosphoric acid for enrichment of rare earth elements

Bona Deng[1], Guanghui Li[1,*], Jun Luo[1,*], Qing Ye[1], Mingxia Liu[1], Mingjun Rao[1], Tao Jiang[1]

Lukas Bauman[2], Boxin Zhao[2]

1, School of Minerals Processing & Bioengineering, Central South University, Changsha, Hunan 410083, China

2, Department of Chemical Engineering, University of Waterloo, Waterloo, Ontario N2L3G1, Canada

[*]Corresponding authors:

Dr. Guanghui Li

Peace Building, RM 253, Central South University, Changsha, Hunan 410083, China

Email: liguangh@csu.edu.cn, Tel: +86-731-88830542

Dr. Jun Luo

Peace Building, RM 242, Central South University, Changsha, Hunan 410083, China

Email: luojun2013@csu.edu.cn, Tel: +86-731-88830542

Both corresponding authors contributed this paper equally.

Selectively leaching the iron-removed bauxite residues with phosphoric acid for enrichment of rare earth elements

Bona Deng[1], Guanghui Li[1,*], Jun Luo[1,*], Qing Ye[1], Mingxia Liu[1], Mingjun Rao[1], Tao Jiang[1]

Lukas Bauman[2], Boxin Zhao[2]

1, School of Minerals Processing & Bioengineering, Central South University, Changsha, Hunan 410083, China

2, Department of Chemical Engineering, University of Waterloo, Waterloo, Ontario N2L3G1, Canada

Abstract

Bauxite residue (BR) is a hazardous industrial waste and also becomes an important reserve of rare earth elements (REE). An elegant process for achieving separation of REEs against silica from an iron-removed BR was established in this paper through selective leaching of silica with simultaneous enrichment of REEs. It was found that the phosphoric acid performed better than other acids (HNO_3, HCl) for multiple REEs enrichment. The ideal conditions for the leaching process was determined through response surface methodology (RSM) to be H_3PO_4 concentration of 1.2 mol/L, L/S ratio of 11mL/g and leaching temperature of 40^oC. 82.3% SiO_2 in iron-removed BR was leached out while the REEs (La_2O_3, Ce_2O_3, Sc_2O_3 and Y_2O_3) remained in the leached residue with recovery of more than 98%. La_2O_3 and Ce_2O_3 were proved to be in lattice replacement within the acid-resistant pervoskite and thus remained in the leached residue. Only part of Sc_2O_3 and Y_2O_3 entered into pervoskite and the remainder was trapped in the aluminosilicate minerals. The enrichment of Sc_2O_3 and Y_2O_3 in phosphoric acid leaching process

was related to the low acidity of H_3PO_4 solution.

Key words: Bauxite residue; Rare earth elements; Enrichment; Silica; Acid leaching

1. Introduction

Rare earth elements (REEs) are essential to modern society with a wide application in the fields of global communications, transportation, medicine, energy and surveillance, etc. [1], as a result, the global market for them has steadily increased. Recently, close attention has been paid to processes that reclaim REEs from electronic wastes [2-4] and secondary resources such as coal ash [5], bauxite and kaolin residue and other industrial wastes [6-7].

Bauxite residue is a hazardous byproduct generated in alumina digestion process of bauxite with about 120 million tons generation annually [8]. Although the main application of bauxite residue is building materials production [9-10] and environmental treatment [11-13], bauxite residue has become an importance secondary resource due to various valuable components such as Fe_2O_3, Al_2O_3, CaO, TiO_2 and REEs trapped within [14]. It is reported that REEs make up as much as 500-1700 mg/kg of the bauxite residue and generally hydrometallurgical processes are used for their extraction [15]. The most applicable method for extracting REEs from bauxite residue is direct leaching with mineral acids [16-17]. The major drawback of this approach is the dissolution of the major elements in bauxite residues which further complicates downstream processes used for REE extraction [18]. Therefore to increase the viability of REE extraction, increasing the selectivity of the acid leaching for REEs along with minimizing the solubilization of impurities is needed.

Selective recovery of REEs has been extensively researched. Some of the processes that

have received attention include bioleaching [19-20] and leaching with highly acidic ionic liquids [21], which exhibit enhanced performance in selectively recovering REEs. Other approach that has also received concentrated investigation is the combination of pyrometallurgical and hydrometallurgical process. Generally prior to the leaching process, bauxite residue either undergoes smelting or reductive roasting to remove iron, the feasibility of this process was confirmed by Borra et al [22] and Li et al [23-24]. After REEs leaching, solvent extraction or ion exchange or some combination thereof is usually performed to recover REEs from the acid leachate [25-27]. However, it is found that any significant amount of dissolved silicon (about 2g/L) in the acid solution can cause the formation of insoluble gel precipitates [28], and further result in emulsification making REEs extraction difficult. Therefore, the separation of REEs against silica in leachate is of great significance for REEs extraction.

According to literatures, different approaches have been conducted to separate REEs against silica, and this is often achieved by suppressing silica dissolution prior to REEs leaching. The sulfation followed by roasting process [29] or highly concentrated acid [30] are used to suppress the formation of the soluble silica monomers (e.g., H_4SiO_4) and consequently silica take the form of insoluble silicon oxides. After water leaching, the REEs are easily dissolved while the silica was remained in the residues. But these methods are restricted by the high energy consumption of the roasting process or the high cost of concentrated acids. In our previous study [23], a more elegant and low-energy consumption process was proposed to achieve the separation between SiO_2 and Sc_2O_3 in bauxite residues. This process used phosphoric acid at low concentration and at ambient temperature. Opposite to the researches mentioned-above, silica in the bauxite residue

was leached out while Sc_2O_3 was reserved in leached residues. The obtained high content Si-bearing leachate can be further processed to produce high-value white carbon product.

Response surface methodology (RSM) is a useful mathematical and statistical technique to optimize and evaluate interactive effects of several independent variables on the response, and has been applied in numerous chemical and biochemical processes [31]. This methodology is more practical compared to the traditional approaches since it includes the linear, quadratic, and interaction of each factor and can depict the overall effects of the parameters on the process [32].

At present, it has been recognized that the reductive roasting process followed by magnetic separation is an efficient technique for iron recovery from various types of mineral ores, especially the refractory complex ores such as bauxite residues [24], lateric nickel ore [33], oolitic hematitie [34] and ludwigite [35], etc. In our recent work, it was surprisingly found out that multiple REEs including Sc_2O_3, La_2O_3, Ce_2O_3 and Y_2O_3 were enriched in the bauxite residues after preliminary iron recovery through reductive roasting and magnetic separation process. To make a comprehensive recovery of these multiple REEs, it was necessary to achieve the separation of REEs against silica in advance. The feasibility of selectively removing silica from the iron-removed bauxite residues with simultaneously enrichment of REEs was investigated using different acid leaching agents such as HCl, HNO_3 and H_3PO_4. The response surface methodology (RSM) was applied to optimize the leaching process and obtain the optimal leaching conditions. Furthermore, the distinguished behaviors of REEs in various acid solutions were examined and thus the enrichment mechanism of these various REEs was ascertained.

2. Material and methods

2.1. Materials

Based on our previous study [23], the iron-removed bauxite residue (BR) used in this study was collected after the optimized reductive roasting and magnetic separation process (5wt.% sodium sulfate and 10wt.% sodium carbonate, roasting at 1100^{o}C, magnetic intensity with 0.1T). In this process the iron in bauxite residues was extracted at efficiency of 90%.

The chemical compositions of the original BR and iron-removed BR are shown in Table 1. The main REEs in BR are La_2O_3, Ce_2O_3, Sc_2O_3 and Y_2O_3. As seen below the mass fraction of iron in original BR was significantly reduced from 21wt% to 3.5wt% after the iron removal treatment while the concentration of the Al_2O_3, SiO_2, CaO and TiO_2 as well as REEs were increased. 90% of the REEs such as La_2O_3, Ce_2O_3, Sc_2O_3 and Y_2O_3 were recovered in the iron-removed bauxite residue.

Table 1 Main chemical compositions of bauxite residue and iron-removed bauxite residue/wt.%

Sample	TFe	Al_2O_3	SiO_2	Na_2O	CaO	TiO_2	La_2O_3	Ce_2O_3	Sc_2O_3	Y_2O_3	LOI
BR	21.0	18.7	12.2	6.6	13.3	5.2	0.0117	0.0534	0.0086	0.0178	14.03
Iron-removed BR	3.5	26.8	19.8	11.27	18.79	7.64	0.0168	0.0863	0.0147	0.0257	9.54

LOI: loss on ignition

2.2. Methods

2.2.1 Acid leaching

An electro-thermostatic water bath equipped with a stir bar was used for acid leaching if the temperature required was below 100^{o}C, while an autoclave was used if the temperature required

was higher than 100°C. The autoclave was equipped with six 100mL pots and incorporated a temperature controller [36]. Silicon oil was used as heating medium so that temperature can be adjusted in the range of 100-280°C. As the acid leaching progressed after a given period of time, the resultant thick slurry would be diluted and filtrated, and further scrubbed with distilled water. The filtrating cake was finally dried in an oven at 105°C for about 4 h before analysis.

The percentage extraction of SiO_2 and REEs was calculated based on the following equations:

$$\varepsilon(\mathrm{M}, \%) = \gamma \times \frac{\beta}{\alpha} \times 10 \quad (1)$$

$$\gamma = \frac{m_1}{m_0} \times 100 \quad (2)$$

where $\varepsilon(\mathrm{M})$ represents the leaching ratio of SiO_2 and REEs, %; γ is the yield of the leached residue, %; α is the content of SiO_2 or REEs in original bauxite residue or iron-removed bauxite residue; β is the content of SiO_2 or REEs in the leached residue, %.

2.2.2 Experimental design for the acid leaching process

In our previous study [23], it was confirmed that the acid concentration, liquid to solid ratio (L/S) and leaching temperature were the essential factors influencing the leaching ratio of different components in bauxite residues. In order to achieve the selective removal of SiO_2 and enrichment of REEs in the leaching process, the response surface methodology (RSM) [32] was introduced to investigate the individual and interaction effects of these experimental factors and thus obtain the optimal leaching conditions. The selected factors and their levels were shown in Table 2.

Table 2 Experimental factors and their selected levels

		Acid concentration (mol/L)	Liquid to solid ratio (mL/g)	Leaching temperature (^{o}C)
Low level	Coded	-1	-1	-1
	Uncoded	1.0	5	25
Middle level	Coded	0	0	0
	Uncoded	1.5	10	45
High level	Coded	1	1	1
	Uncoded	2.0	15	65

2.2.3 Test techniques

Chemical compositions of the solid samples were determined by an X-ray fluorescence spectrometer (XRF, PANalytical, Axios mAX, Netherlands), while the mineral compositions were confirmed using a X-ray diffraction (XRD, RIGAKU, D/Max 2500, Japan) under the conditions of radiation: Cu Kα, tube current and voltage: 250 mA, 40 kV, scanning range: 10-80° (2θ), step size: 0.02°(2θ) and scanning speed: 8°(2θ)/min. The contents of rare earth elements were ascertained by plasma emission spectrometer (ICP-AES, Icap7400 Radial, America).

3. Results and Discussion

3.1. Leaching on iron-removed bauxite residue with different acids

The effects of different acids on the leaching of SiO_2 and multiple REEs in the iron-removed BR were investigated. The conditions were fixed at a leaching temperature of 25^{o}C, leaching time of 60 min and liquid to solid ratio of 10 mL/g. The results were exhibited in Fig.1-Fig.2.

The common minerals acids such as HCl, HNO_3, H_2SO_4 and H_3PO_4 were used, but it was found that the filtration was difficult to progress when using H_2SO_4 to treat iron-removed BR, which should be due to the generation of $CaSO_4$ in the filtrating process. Thus only the leaching results of HCl, HNO_3, and H_3PO_4 were taken into consideration in this study. The leaching ratio of SiO_2 increased with increasing acid concentration of the HCl, HNO_3, and H_3PO_4, while REEs behaved quite variably. La_2O_3 and Ce_2O_3 showed almost no dissolution, and their leaching ratios were less than 3% over the course of the experiment regardless of the type of acid used. Sc_2O_3 and Y_2O_3 were behaved similarly and dissolved gradually in response to the concentration increase of HCl and HNO_3. The leaching ratios were 77% and 35% for Sc_2O_3 and Y_2O_3 respectively at HNO_3 concentration of 4 mol/L. When H_3PO_4 was used as the leaching agent, Sc_2O_3 and Y_2O_3 showed limited dissolution with a leaching ratio less than 3% at acid concentration lower than 1.5mol/L. Under the same conditions SiO_2 showed a leaching ratio upwards of about 75%. After continuously increasing the concentration of H_3PO_4, Sc_2O_3 and Y_2O_3 began to gradually dissolve and their leaching ratio maximized at 55% and 27% respectively for a H_3PO_4 concentration of 4 mol/L.

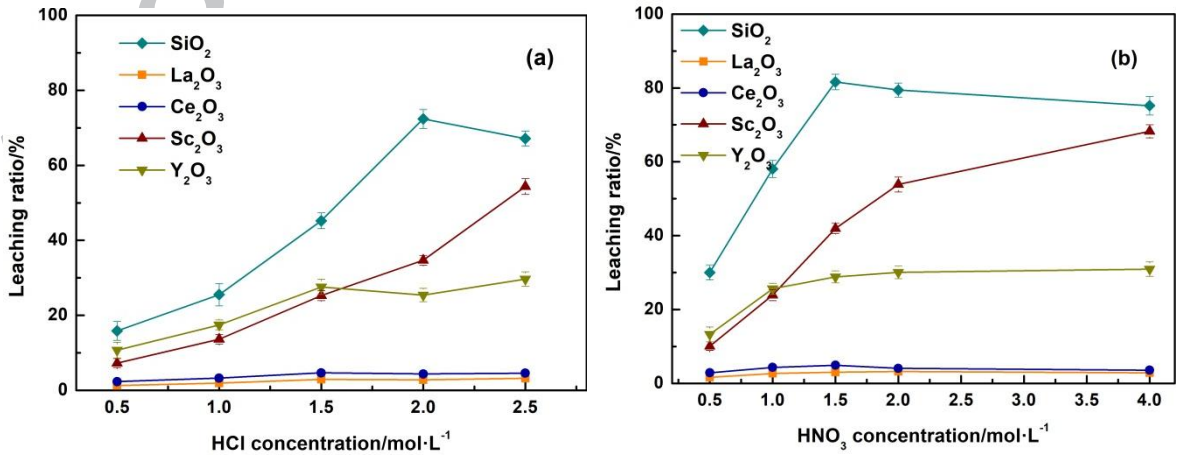

Fig.1 Effect of HCl and HNO_3 concentration on leaching ratio of SiO_2 and REEs from the iron-removed bauxite residue

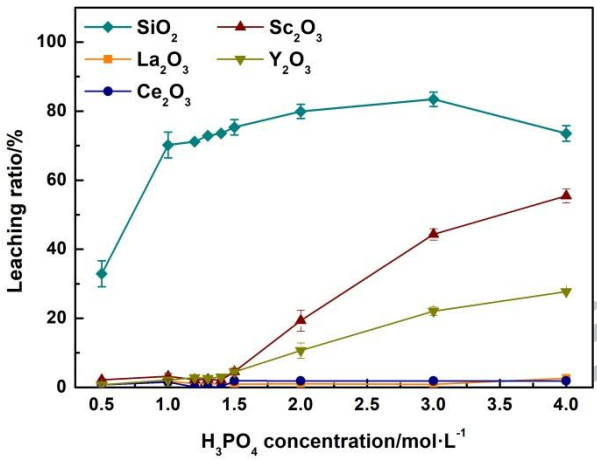

Fig.2 Effect of H_3PO_4 concentration on leaching ratio of SiO_2 and REEs from the iron-removed bauxite residue

The above results confirmed that the selectively extracting SiO_2 while reserving La_2O_3 and Ce_2O_3 in iron-removed BR can be achieved using any one of the three acids, but only H_3PO_4 can meet the requirement while taking into account of enrichment of Sc_2O_3 and Y_2O_3. A superb separation of SiO_2 over Sc_2O_3 and Y_2O_3 can be achieved when H_3PO_4 concentration was lower than 1.5 mol/L. Under this condition, the leaching ratio of SiO_2 reached about 75% while less than 3% of La_2O_3, Ce_2O_3, Sc_2O_3 and Y_2O_3 were solubilized.

3.2 Optimization of phosphoric acid leaching process on iron-removed bauxite residue

3.2.1 Box-Behnken design (BBD) design

Unlike the traditional factorial experiment which needs to investigate each collocation of experimental factors, a minimum number of experiments are required in RSM to ascertain both

of linear and interaction effect of the experimental factors. Through RSM, the results can fit in a second order equation ($Y = \beta_0 + \sum_{i=1}^{3} \beta_i X_i + \sum_{i<j}^{3} \beta_{ij} X_i X_j + \sum_{i=1}^{3} \beta_{ii} X_i^2$) for the response.

In this section, the optimal phosphoric acid leaching conditions for the removal of SiO_2 and enrichment of La_2O_3, Ce_2O_3, Sc_2O_3 and Y_2O_3 from iron-removed BR were determined. As confirmed in 3.1, La_2O_3 and Ce_2O_3 in the iron-removed BR remained un-dissolved while Sc_2O_3 and Y_2O_3 were gradually solubilized with increasing H_3PO_4 concentration. Therefore, the difference value between the leaching ratio of SiO_2 and Sc_2O_3, Y_2O_3 was regarded as the response to represent the separation efficiency (SE) for the phosphoric acid leaching process. The equation was given in Eq. (3).

$$\text{Separation efficiency (SE, \%)} = \varepsilon_{SiO_2} - \varepsilon_{Sc_2O_3} - \varepsilon_{Y_2O_3} \quad (3)$$

where SE represents the response, ε_{SiO_2}, $\varepsilon_{Sc_2O_3}$ and $\varepsilon_{Y_2O_3}$ is the respective leaching ratio of SiO_2, Sc_2O_3 and Y_2O_3, %.

In response surface modeling, Box-Behnken design (BBD) is typically applied to design the experiments. As confirmed in the previous study [23], the dominant experimental factors were H_3PO_4 concentration, L/S ratio and leaching temperature. Table 3 shows the experimental scheme and corresponding leaching results based on BBD design. Owing to the regression of the coefficient through BBD, the final equation for SE can be given in Eq. (4).

$$SE = -274.22+269.05A+24.51B+2.80C-9.25AB-0.10AC-0.01BC-67.62A^2-0.59B^2-0.03C^2 \quad (4)$$

where A, B, C are the linear effect of H_3PO_4 concentration, L/S ratio and leaching temperature; AB, AC, BC are interaction effects of these factors; A^2, B^2, C^2 represents quadratic effects of each factor.

Table 3 BBD design matrix for the leaching ratio of SiO_2, Sc_2O_3 and Y_2O_3 and separation efficiency (SE)

No.	A- H_3PO_4 conc. (mol/L)		B- L/S ratio (mL/g)		C: Leaching temperature, (^oC)		ε_{SiO_2}	$\varepsilon_{Sc_2O_3}$	$\varepsilon_{Y_2O_3}$	*SE*
	Coded	Uncoded	Coded	Uncoded	Coded	Uncoded				
1	-1	1	-1	5	0	45	45.23	0.35	0.51	44.37
2	0	1.5	0	10	0	45	78.27	1.52	1.36	75.39
3	0	1.5	1	15	1	65	70.28	15.84	17.97	36.47
4	0	1.5	-1	5	1	65	50.27	1.36	2.1	46.81
5	-1	1	0	10	1	65	58.57	0.81	1.27	56.49
6	0	1.5	0	10	0	45	79.67	1.31	1.87	76.49
7	0	1.5	-1	5	-1	25	61.34	1.07	2.37	57.9
8	0	1.5	1	15	-1	25	85.15	16.35	18.47	50.33
9	0	1.5	0	10	0	45	79.98	2.03	3.07	74.88
10	1	2	-1	5	0	45	68.23	2.31	3.57	62.35
11	0	1.5	0	10	0	45	78.52	1.15	2.16	75.21
12	1	2	0	10	-1	25	79.04	20.16	22.05	36.83
13	0	1.5	0	10	0	45	79.03	1.56	2.27	75.2
14	1	2	1	15	0	45	90.37	65.37	27.86	-2.86
15	1	2	0	10	1	65	65.23	21.23	23.15	20.85
16	-1	1	0	10	-1	25	70.23	0.87	1.01	68.35
17	-1	1	1	15	0	45	75.89	1.92	2.35	71.62

3.2.2 ANOVA analysis of the model

The analysis of variance (ANOVA) with F-value test can be used to evaluate the significance of a model [37]. As shown in Table 4, the F-value of 91.98 means the established model fits well and the model terms (except of AC and BC) are significant since their p-values are basically less than 0.05. Fig. 3 shows the importance of the liner, interaction and square effects of experimental factors with respect to the sum of squares obtained from ANOVA. As the value of sum of squares increases, the significance of the experimental factors in the process also increases. It was seen that the square effect of H_3PO_4 concentration, linear effect of H_3PO_4 concentration and interaction effect between H_3PO_4 concentration and L/S ratio were dominant.

Determination coefficient (R^2) describes the amount of variation in response that can be explained by the model [38-39]. In this case, the determination coefficient (R^2) of the established model is 0.9916, indicating 99.16% of the total variation of response can be explained by the model given in Eq. (4). It was evident that the model established in this study was valid and accounted for as significant portion of the variation present.

Table 4 ANOVA for response surface quadratic model

Source	Sum of Squares	df	Mean Square	F Value	p-value Prob > F
Model	7926.66	9	880.74	91.98	< 0.0001
A-H_3PO_4 conc.	1911.47	1	1911.47	199.62	< 0.0001
B-L/S ratio	390.18	1	390.18	40.75	0.0004
C-Leaching temperature	348.35	1	348.35	36.38	0.0005
AB	2137.21	1	2137.21	223.20	< 0.0001

AC	4.24	1	4.24	0.44	0.5269
BC	1.92	1	1.92	0.20	0.6680
A^2	1203.39	1	1203.39	125.68	< 0.0001
B^2	904.69	1	904.69	94.48	< 0.0001
C^2	700.48	1	700.48	73.15	< 0.0001
Residual	67.03	7	9.58		
Lack of Fit	65.50	3	21.83	57.12	0.0010
Pure Error	1.53	4	0.38		
Corn Total	7993.69	16			

R^2= 0.9916

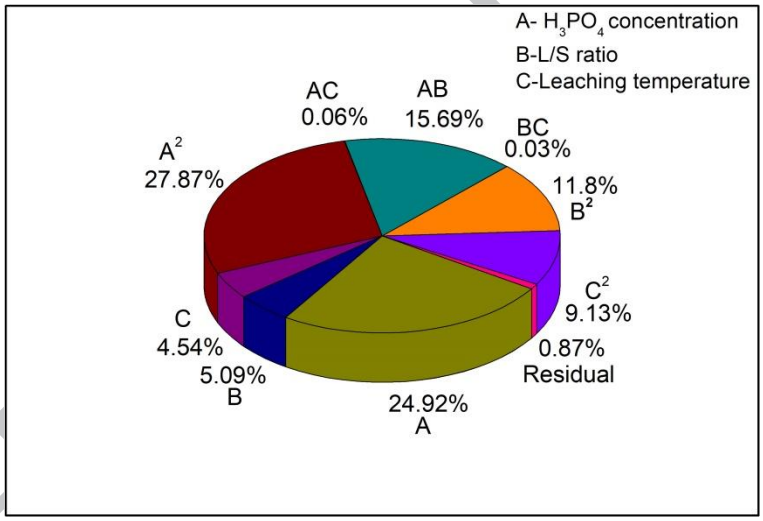

Fig. 3 Significance of different model terms via adjusted sum of squares

3.2.3 Combined effects of the experimental factors on the response

In order to obtain further insight of how H_3PO_4 concentration, L/S ratio and leaching temperature influence the separation efficiency of the phosphoric acid leaching process, the 3D mesh diagrams which showed the combined effects of the experimental variables within the

design space were plotted as shown in Fig. 4. As the interaction effect of each two variables was addressed precisely and separately, the optimal process conditions can thus be obtained [40]. The separation efficiency was optimized and reached the maximum of about 80% as the optimal H_3PO_4 concentration, L/S ratio and leaching temperature were determined to be 1.2 mol/L, 11 mL/g and 40^oC, respectively.

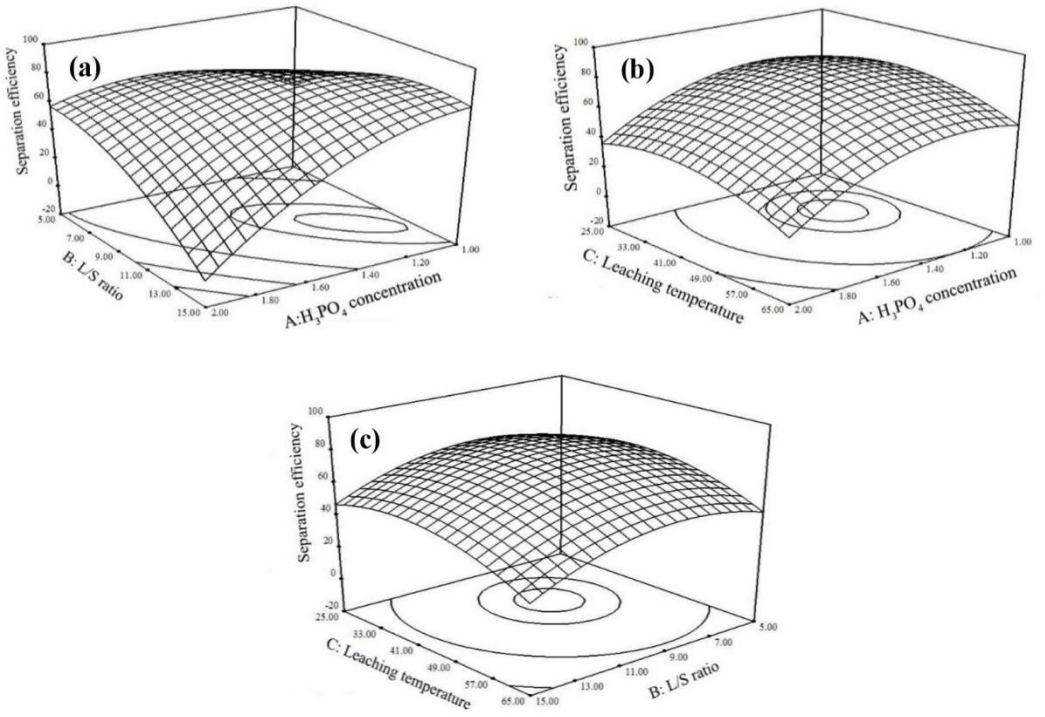

Fig. 4 3D plot depicting the combined effect of experimental factor on the separation efficiency(SE) of phosphoric acid leaching process: (a) effects of H_3PO_4 concentration and L/S ratio, (b) effects of H_3PO_4 concentration and leaching temperature, (c) effects of liquid to L/S ratio and leaching temperature

Once the optimal conditions were found from the RSM, tests under these conditions were performed to assess the accuracy of the predictions. The leaching ratio of the main components

was shown in Table 5. The yield of the leached residue was about 80.2%, and leaching ratio of SiO_2 attained 82.3% while the rare earth elements La_2O_3, Ce_2O_3, Sc_2O_3 and Y_2O_3 experienced almost no leaching, with a leaching ratio less than 2%. The separation efficiency (ε_{SiO_2}- $\varepsilon_{Sc_2O_3}$- $\varepsilon_{Y_2O_3}$) was found to be 79.5%, which is nearly identical to predicted value obtained by RSM. From these results it can be concluded that the RSM analysis accurately modeled the process and the optimal conditions found from it were valid.

Table 5 The actual leaching results of iron-removed bauxite residue under predicted conditions by RSM

Leaching ratio/%					Yield	REEs content in leached residue/%			
SiO_2	La_2O_3	Ce_2O_3	Sc_2O_3	Y_2O_3		La_2O_3	Ce_2O_3	Sc_2O_3	Y_2O_3
82.3	0.65	1.02	1.05	1.84	86.2	0.0190	0.0840	0.0167	0.0290

3.3 Enrichment mechanism of REEs in acid leaching process

As confirmed in above sections, the leaching performance of the La_2O_3 and Ce_2O_3 in iron-removed BR was different from that of Sc_2O_3 and Y_2O_3; thereof their enrichment mechanism was also distinguished. Since REEs content in BR is extremely low and it is impossible to directly detect their bearing mineral phases through the traditional methods such as XRD, SEM and EDS, their enrichment mechanism was deduced and elucidated through their leaching performance.

3.3.1 Enrichment mechanism of La_2O_3 and Ce_2O_3

The XRD patterns of the iron-removed BR and its leached residues are shown in Fig. 5. It was shown that dominant minerals in iron-removed BR were sodium aluminosilicate ($NaAlSiO_4$), grossular ($Ca_3Al_2Si_3O_{12}$) and perovskite ($CaTiO_3$). The perovskite ($CaTiO_3$) proved acid-resistant and its peaks in the leached residues were dramatically increased corresponding to the increase of acid concentration. These Al- and Si-bearing minerals in the iron-removed BR can be seen as $MeO_{n/2} \cdot xAl_2O_3 \cdot ySiO_2$ (Me = Ca, Na), and could be gradually dissolved in the acid solution. As the H_3PO_4 concentration was low (less than 1.5M), the grossular ($Ca_3Al_2Si_3O_{12}$) contacted with acid solution and transformed into calcium aluminum oxides ($Ca_2Al_3O_6$) as the containing SiO_2 was solubilized. The Na_2O and SiO_2 in sodium aluminosilicate ($NaAlSiO_4$) were also dissolved in the H_3PO_4 liquor while Al_2O_3 reacted with H_3PO_4 liquor to form insoluble $AlPO_4$. These newly-formed $AlPO_4$ would cover on the surface of the original sodium aluminosilicate ($NaAlSiO_4$), and prohibited its further dissolving. As a result, there were still some sodium aluminosilicate ($NaAlSiO_4$) undissolved and left in the leached residues. The XRD patterns have confirmed this result and the peaks of $AlPO_4$ and sodium aluminosilicate ($NaAlSiO_4$) were detected in the leached residues at H_3PO_4 concentration of 1.5M. With increasing the acid concentration to 4M, it was seen that calcium aluminum oxides ($Ca_2Al_3O_6$) and $AlPO_4$ can be dissolved in the strong acid solution and their peaks finally disappeared. There were no peaks of Al- and Si-bearing minerals except perovskite ($CaTiO_3$) existed in the leached residues of H_3PO_4

concentration of 4M. The ionization reactions of phosphoric acid occur stepwise as shown in Eq. (5)-(7) and reactions of minerals dissolving in acid solution are described in Eq. (8)-(11).

As shown in previous section that La_2O_3 and Ce_2O_3 in iron-removed BR remained intact despite increasing H_3PO_4 concentration to 4mol/L (see Fig. 2), it was thus ascertained that La_2O_3 and Ce_2O_3 in the iron-removed BR were dominantly existed in the perovskite lattice. As a result, La_2O_3 and Ce_2O_3 in the iron-removed BR avoided dissolution in the subsequent leaching process. Since Sc_2O_3 and Y_2O_3 in iron-removed BR can be dissolved corresponding to the increase of acid concentration, their enrichment cannot due to their existence in the perovskite lattice.

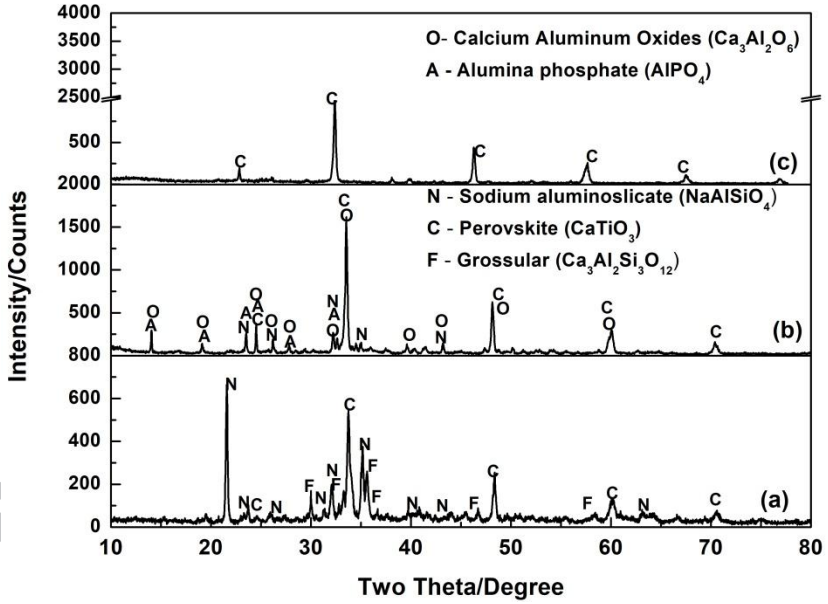

Fig.5 XRD patterns of iron-removed BR and their leached residues: (a) iron-removed BR; (b) leached residue at 1.5 M H_3PO_4; (c) leached residue at 4.0 M H_3PO_4

⇌ - (5)

- ⇌ - (6)

$$\text{-} \rightleftharpoons \text{-} \quad (7)$$

$$\text{p} \quad \text{-} \quad \text{m} \quad _4 \quad _{(aq)} \quad (8)$$

$$Ca_3Al_2Si_3O_{12} + 6H_2O = Ca_3Al_2O_6 + 3H_4SiO_{4(aq)} \quad (9)$$

$$\text{m} \quad _4 \quad = \quad \text{-} \quad (10)$$

$$Ca_3Al_2O_6 + 12H^+ = 3Ca^+ + 2Al^{3+} + 6H_2O \quad (11)$$

3.4.2 Enrichment mechanism of Sc_2O_3 and Y_2O_3

As confirmed in our previous research [23], Sc_2O_3 in the iron-removed BR was hypothesized in the form of metal oxide and its enrichment was believed due to its dissolution pH^0 being lower than the solution pH in the phosphoric acid leaching process. Here, it was also hypothesized that Y_2O_3 would take the form of metal oxide trapped in the aluminosilicate minerals in the iron-removed BR. The dissolution pH^0 of Y_2O_3 was calculated as shown in Fig.6. It was confirmed that this value was close to 10, being much higher than the pH of H_3PO_4 solution during the leaching process, which indicated Y_2O_3 would be easily dissolved in H_3PO_4 solution. This result was in conflict with the fact that Y_2O_3 in iron-removed BR was not dissolved in phosphoric acid under specified concentrations. Therefore, Y_2O_3 cannot exist as free metal oxides within iron-removed BR. Correspondingly, the enrichment mechanism of Y_2O_3 was not related with its dissolution pH^0.

On the other hand, it was seen from Fig.1 and Fig.2, Y_2O_3 behaved closely similar with Sc_2O_3 in the leaching process, it was much convincing that Y and Sc in iron-removed BR occurred in isomorphism. As they would not be in lattice replacement with perovskite nor as free metal oxide

in iron-removed BR, they should be within the lattice of the aluminosilicate minerals, namely sodium aluminosilicate ($NaAlSiO_4$) and grossular ($Ca_3Al_2Si_3O_{12}$) in iron-removed BR. As demonstrated in Fig.5 that, the grossular ($Ca_3Al_2Si_3O_{12}$) has dominantly transformed into calcium aluminum oxides ($Ca_2Al_3O_6$) while sodium aluminosilicate ($NaAlSiO_4$) transformed into $AlPO_4$ in the leaching process with H_3PO_4 concentration less than 1.5mol/L. The H^+ in the acid solution was mainly to solubilize SiO_2 and Na_2O while most of CaO and Al_2O_3 in the iron-removed BR were not dissolved and reserved. After the acid concentration was continuously increased, the calcium aluminum oxides ($Ca_2Al_3O_6$), sodium aluminosilicate ($NaAlSiO_4$) and $AlPO_4$ were further dissolved and their peaks in the leached residues vanished. Therefore, it can be deduced that Sc and Y in the iron-removed BR mainly co-existed within the atom of Ca and Al in the aluminosilicate minerals. As these Ca- and Al- bearing aluminosilicate in the iron-removed BR were solubilized, Sc and Y were exposed and got solubilized as well.

Meanwhile, through comparing the leaching performance of Y_2O_3 and Sc_2O_3 at different acids (seen in Fig.1-Fig, 2), it was convincing that their enrichment in the H_3PO_4 leaching process was likely related to the solution acidity. As demonstrated in Fig.6 that the pH of H_3PO_4 solution was much higher than that of HCl and HNO_3 under identical leaching conditions. This implies the Ca- and Al- bearing aluminosilicate minerals were easily dissolved in HCl and HNO_3 versus H_3PO_4. As a result, Sc_2O_3 and Y_2O_3 in iron-removed BR were more likely to be leached out when using HCl and HNO_3 to treat the iron-removed BR.

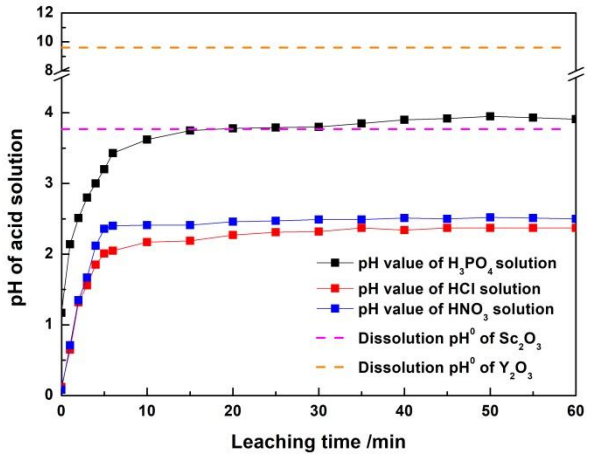

Fig. 6 Variation of solution pH during the leaching process and the dissolution pH^0 of Sc_2O_3 and Y_2O_3 (Temperature of 25°C, acid concentration of 1.0mol·L^{-1}, liquid to solid ratio of 10mL/g)

3.4.3 Validation of REEs enrichment mechanism

To further validate the proposed enrichment mechanism of REEs, a high-concentration acid leaching process was conducted on the iron-removed BR, and the leaching performance of REEs were analyzed in comparison with that in BR. The conditions were fixed at 8 mol/L of HNO_3, a liquid to solid ratio of 10 mL/g and leaching time of 60min.

It was found in Fig.7 that the no obvious dissolution of La_2O_3 and Ce_2O_3 was observed at 25°C with acid concentration of 8mol/L when only perovskite was detected in the leached residues. As leaching temperature reached 200°C, the leaching ratio of La_2O_3 and Ce_2O_3 attained 90% when the perovskite has been decomposed and transformed into anatase (TiO_2). It can be seen that a positive correlation existed between the REEs (La_2O_3 and Ce_2O_3) leaching and perovskite dissolving. These results strongly verified that La_2O_3 and Ce_2O_3 entered the perovskite lattice during the reductive roasting of BR.

Also, it was shown in Fig.7 that leaching ratio of Sc_2O_3 and Y_2O_3 reached upwards of 70%

and 30% respectively at 25°C with acid concentration of 8mol/L when the leached residue was made up of perovskite. This indicates that the undissolved Sc_2O_3 (30%) and Y_2O_3 (70%) in iron-removed BR existed in the lattice of perovskite, and thus the dissolved Sc_2O_3 (70%) and Y_2O_3 (30%) resided in aluminosilicates minerals. As the leaching temperature was elevated to 200°C, perovskite decomposed and the trapped Sc_2O_3 and Y_2O_3 were released, and as a result the leaching ratios of Sc_2O_3 and Y_2O_3 significantly increased and this value attained 90% at last. The part of Sc_2O_3 and Y_2O_3 trapped in perovskite cannot be dissolved in the acid leaching while the other part trapped in aluminosilicates would be easily solubilized. Therefore, in order to investigate the enrichment mechanism of Sc_2O_3 and Y_2O_3 in the iron-removed BR during acid leaching, it was the key to investigate the enrichment of Sc_2O_3 and Y_2O_3 trapped in aluminosilicates, and this has been explained in the above section.

After removal of silica and enrichment of REEs from BR, the obtained leached residues become a superb material for REEs extraction. This material can be further processed with acid leaching and solvent extraction to extract REEs without interference by emulsification primarily caused by silica.

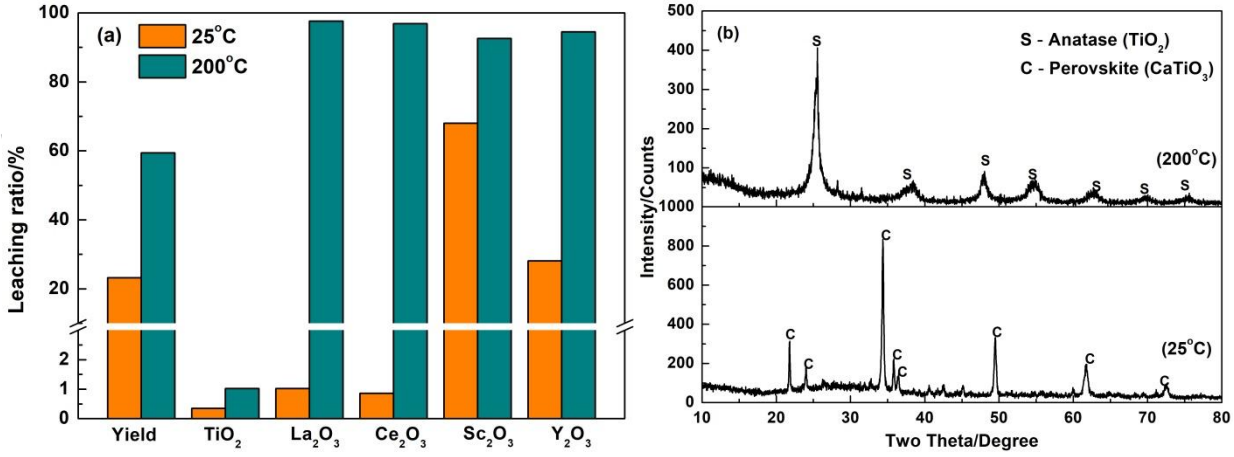

Fig. 7 Leaching results of iron-removed BR using concentrated acid (a) and the XRD patterns of the leached residues (b)

4. Conclusions

An excellent enrichment of multiple rare earth elements and their simultaneous separation against silica from the iron-removed BR was achieved in this study, and the conclusions were as follows:

(1) Among the three common acids (HCl, HNO_3, H_3PO_4), only H_3PO_4 was able to achieve the separation of REEs (e.g. La_2O_3, Ce_2O_3, Sc_2O_3 and Y_2O_3) against silica in the iron-removed bauxite residues, this was obtained through selective removal of silica and simultaneously reserve of multiple REEs (La_2O_3, Ce_2O_3, Sc_2O_3 and Y_2O_3) in the leached residues.

(2) RSM was successfully applied to optimize the phosphoric acid leaching process on iron-removed bauxite residues and the optimal conditions obtained were H_3PO_4 concentration of 1.2mol/L, L/S ratio of 11mL/g and leaching temperature of 40^{o}C, respectively. The actual leaching experiment verified that leaching ratio of SiO_2 attained 82.3% while minimal La_2O_3, Ce_2O_3, Sc_2O_3 and Y_2O_3 were almost not leached out with the leaching ratios less than 2% under these predicted conditions.

(3) La_2O_3 and Ce_2O_3 entered the lattice of pervoskite during reductive roasting of bauxite residue. As a result, they avoided dissolution in subsequent leaching process since perovskite was acid-resistant in ambient atmosphere.

(4) Only about 30% Sc_2O_3 and 70% Y_2O_3 entered into the lattice of perovskite, and the

other 70% Sc_2O_3 and 30% Y_2O_3 mainly co-existed within the atom of Ca and Al of the aluminosilicate minerals in the iron-removed BR. Due to the lower acidity of H_3PO_4 than HCl and HNO_3, the Sc, Y-trapping aluminosilicate minerals were difficult to solubilize in H_3PO_4 solution and thus Sc_2O_3 and Y_2O_3 were enriched in the leached residues.

The process used in this study to achieve separation of REEs against silica is low energy consumption and low cost, and convincing to be applicable on other REEs-bearing minerals resources for REEs enrichment and extraction.

Acknowledgements

The authors wish to express their thanks to the National Natural Science Foundation of China (No.51234008 and 51174230) for the financial support of this research. This work was also financially supported by Co-Innovation Center for Clean and Efficient Utilization of Strategic Metal Mineral Resources.

Declarations of interest: none.

References

[1] J.H. Pan, C.C. Zhou, M.C. Tang, S.S. Cao, C. Liu, N.N. Zhang, M.Z. Wen, Y.L. Luo, T.T. Hu, W.S. Ji, Study on the modes of occurrence of rare earth elements in coal fly ash by statistics and a sequential chemical extraction procedure, Fuel. 237 (2019) 555-565. https://doi.org/10.1016/j.fuel.2018.09.139

[2] A. Walton, H. Yi, N.A. Rowson, J.D. Speight, V.S.J. Mann, R.S. Sheridan, A. Bradshaw, I.R.

Harris, A.J. Williams, The use of hydrogen to separate and recycle neodymium-iron-boron-type magnets from electronic waste, J. Clean. Prod. 104 (2015) 236-241. https://doi.org/10.1016/j.fuel.2018.09.139

[3] A. Lixandru, I. Poenaru, K. Güth, R. Gauß, O. Gutfleisch, A systematic study of HDDR processing conditions for the recycling of en-of-life Nd-Fe-B magnets, J. Alloys Compd. 724 (2017) 51-61. https://doi.org/10.1016/j.jclepro.2015.05.033

[4] L.S. Wang, X.W. Huang, Y. Yu, L.S. Zhao, C.M. Wang, Z.Y. Feng, D.L. Cui, Z.Q. Long, Towards cleaner production of rare earth elements from bastnaesite in China, J. Clean. Prod. 165 (2017) 231-242. https://doi.org/10.1016/j.jclepro.2017.07.107

[5] X.L. Zeng, J.H. Li, Measuring the recyclability of e-waste: an innovative method and its implications, J. Clean. Prod. 131 (2016) 156-162.https://doi.org/10.1016/j. /j.jclepro.2016.05.055

[6] K. Binnemans, P.T. Jones, B. Blanplain, T. Van Gerven, Y. Pontikes, Towards zero-waste valorization of rare-earth containing industrial process residues: a critical review, J. Clean. Prod. 99 (2015) 17-38. https://doi.org/10.1016/j.jclepro.2015.02.089

[7] Q. Dehaine, L.O. Filippov, Rare earth (La, Ce, Nd) and rare metals (Sn, Nb, W) as by-product of kaolin production, Cornwall: Part 1: Selection and characterisation of the valuable stream, Miner. Eng. 76 (2015) 141-153. https://doi.org/10.1016/j.mineng.2014.10.006

[8] H. Nath, P. Sahoo, A. Sahoo, Characterization of Red Mud treated under high temperature fluidization, Powder. Technol. 269 (2015) 233-239. https://doi.org/10.1016/j.powtec.2014.09.011

[9] Y. Pontikes, G.N. Angelopoulos, Bauxite residue in cement and cementitious applications: Current status and a possible way forward, Resour. Conserv. Recycl. 73 (2013) 53-63.

https://doi.org/10.1016/j.resconrec.2013.01.005

[10] S. Kumar, R. Kumar, A. Bandopadhyay, Innovative methodologies for the utilisation of wastes from metallurgical and allied industries, Resour. Conserv. Recycl. 48 (2006) 301-314. https://doi.org/10.1016/j.resconrec.2006.03.003

[11] M. Gräfe, G. Power, C, Klauber. Bauxite residue issues: III. Alkalinity and associated chemistry, Hydrometallurgy. 108 (2011) 60-79. https://doi.org/10.1016/j.hydromet.2011.02.004

[12] J. Roosen, S. Van Roosendael, C.R. Borra, T. Van Gerven, S. Mullens, K. Binnemans, Recovery of scandium from leachates of Greek bauxite residue by adsorption on functionalized chitosan-silica hybrid materials, Green Chem. 18 (2016) 2005-2013. . https://doi.org/10.1039/c5gc02225h

[13] S. Rai, K.L. Wasewar, D.H. Lataye, J. Mukhopadhyay, C.K. Yoo, Feasibility of red mud neutralization with seawater using Taguchi's methodology, Int. J.Environ. Sci. Technol. 10 (2013) 305-314. https://doi.org/10.1007/s13762-012-0118-7

[14] G. Power, M. Gräfe, C. Klauber, Bauxite residue issues: I. Current management, disposal and storage practices, Hydrometallurgy. 108 (2011) 33-45. https://doi.org/10.1016/j.hydromet.2011.02.006

[15] A. Akcil, N. Akhmadiyeva, R. Abdulvaliyev, P. Meshram, Overview on extraction and separation of REEs from red mud: Focus on scandium, Miner. Process. Extr. Metall. Rev. 39 (2018) 145-151. https://doi.org/10.1080/08827508.2017.1288116

[16] C.R. Borra, Y. Pontikes, K. Binnemans, T. Van Gerven, Leaching of rare earths from bauxite residue (red mud), Miner. Eng. 76 (2015) 20-27. https://doi.org/10.1016/j.mineng.2015.01.005

[17] W.W. Wang, Y. Pranolo, C.Y. Cheng, Recovery of scandium from synthetic red mud leach solutions by solvent extraction with D2EHPA, Sep. Purif. Technol. 108 (2013) 96-102. https://doi.org/10.1016/j.seppur.2013.02.001

[18] B. Onghena, C.R. Borra, T. Van Gerven, K. Binnemans, Recovery of scandium from sulfation-roasted leachates of bauxite esidue by solvent extraction with the ionic liquid betainium bis(trifluoromethylsulfonyl)imide, Sep. Purif. Technol. 176 (2017) 208-219. https://doi.org/10.1016/j.seppur.2016.12.009

[19] Y. Qu, B. Lian, Bioleaching of rare earth and radioactive elements from red mud using Penicillium tricolor RM-10, Bioresour. Technol. 136 (2013) 16-23. https://doi.org/10.1016/j.biortech.2013.03.070

[20] Y. Qu, B. Lian, B.B. Mo, C.Q. Liu, Bioleaching of heavy metals from red mud using Aspergillus niger, Hydrometallurgy. 136 (2013) 71-77. https://doi.org/10.1016/j.hydromet.2013.03.006

[21] P. Davris, E. Balomenos, D. Panias, I. Paspaliaris, Selective leaching of rare earth elements from bauxite residue (red mud), using a functionalized hydrophobic ionic liquid, Hydrometallurgy. 164 (2016) 125-135. https://doi.org/10.1016/j.hydromet.2016.06.012

[22] C.R. Borra, B. Blanpain, Y. Pontikes, K. Binnemans, T. Van Gerven, Smelting of bauxite residue (red mud) in view of iron and selective rare earths recovery, J. Sustain. Metal. 2 (2016)28-37. https://doi.org/10.1016/j.hydromet.2016.06.012

[23] B.N. Deng, G.H. Li, J. Luo, Q. Ye, M.X. Liu, Z.W. Peng, T. Jiang, Enrichment of Sc_2O_3 and TiO_2 from bauxite ore residues, J. Hazard. Mater. 331 (2017) 71-80.

https://doi.org/10.1007/s40831-015-0026-4

[24] G.H. Li, M.X. Liu, M.J. Rao, T. Jiang, J.Q. Zhuang, Y.B. Zhang, Stepwise extraction of valuable components from red mud based on reductive roasting with sodium salts, J. Hazard. Mater. 280 (2014) 774-780. https://doi.org/10.1016/j.jhazmat.2014.09.005

[25] Z.G. Zhao, F. Kubota, N. Kamiya, M. Goto, Selective extraction of scandium from transition metals by synergistic extraction with 2-thenoyltrifluoroacetone and tri-n-octylphosphine oxide, Solvent Extr. Res. Dev. 23 (2016) 137-143. https://doi.org/10.15261/serdj.23.137

[26] B. Gorski, N. Gorski, M. Beer, Extraction of Sc, Y, and lanthanides by quaternary ammonium-salts, Solvent Extr. Ion Exch. 9 (1991) 623-635. https://doi.org/10.1080/07366299108918074

[27] M. Karve, B.K. Vaidya, Selective separation of scandium(III) and yttrium(III) from other rare earth elements using cyanex302 as an extractant, Sep. Sci.Technol. 43 (2008) 1111-1123. https://doi.org/10.1080/01496390801887435

[28] G.H. Li, Q. Ye, B.N. Deng, J. Luo, M.J. Rao, Z.W. Peng, T. Jiang, Extraction of scandium from scandium-rich material derived from bauxite ore residues, Hydrometallurgy. 176 (2018) 62-68. https://doi.org/10.1016/j.hydromet.2018.01.007

[29] C.R. Borra, J. Mermans, B. Blanpain, Y. Pontikes, K. Binnemans, T. Van Gerven, Selective recovery of rare earths from bauxite residue by combination of sulfation, roasting and leaching, Miner. Eng. 92 (2016) 151-159. https://doi.org/10.1016/j.mineng.2016.03.002

[30] R.M. Rivera, B. Ulenaers, G. Ounoughene, K. Binnemans, T. Van Gerven. Extraction of rare

earths from bauxite residue (red mud) by dry digestion followed by water leaching, Miner. Eng. 119 (2018) 82-92. https://doi.org/10.1016/j.mineng.2018.01.023

[31] M. Amini, H. Younesi, N. Bahramifar, A.A.Z. Lorestani, F. Ghorbani, A. Daneshi, M. Sharifzadeh. Application of response surface methodology for optimization of lead biosorption in an aqueous solution by Aspergillus niger. J. Hazard. Mater. 154(2008) 694-702. https://doi.org/10.1016/j.jhazmat.2007.10.114

[32] R. Singh, R. Chadetrik, R. Kumar, K. Bishnoi, D. Bhatia, A. Kumar, N.R. Bishnoi, N. Singh, Biosorption optimization of lead(II), cadmium(II) and copper(II) using response surface methodology and applicability in isotherms and thermodynamics modeling, J. Hazard. Mater. 174 (2010) 623–634. https://doi.org/10.1016/j.mineng.2016.03.002

[33] G.H. Li, T.M. Shi, M.J. Rao, T. Jiang, Y.B. Zhang. Beneficiation of nickeliferous laterite by reduction roasting in the presence of sodium sulfate. Miner. Eng. 32 (2012)19-26. https://doi.org/10.1016/j.mineng.2012.03.012

[34] G.H. Li, S.H. Zhang, M.J Rao, Y.B. Zhang, T. Jiang, Effects of sodium salts on reduction roasting and Fe–P separation of high-phosphorus oolitic hematite ore, Int. J. Miner. Process. 124 (2013) 26-34. https://doi.org/10.1016/j.minpro.2013.07.006

[35] G.H. Li, B.J. Liang, M.J. Rao, Y.B. Zhang, T. Jiang, An innovative process for extracting boron and simultaneous recovering metallic iron from ludwigite ore. Miner. Eng. 56(2014) 57-60. https://doi.org/10.1016/j.mineng.2013.10.030

[36] G.H. Li, J. Luo, T. Jiang, Z.X. Li, Z.W. Peng, Y.B. Zhang. Digestion of alumina from non-magnetic material obtained from magnetic separation of reduced iron-rich diasporic bauxite

with sodium salts. Metals. 6(**2016**) 294. https://doi.org/10.3390/met6110294

[37] J.S. Varsihini C, D. Das, N. Das, Optimization of parameters for cerium(III) biosorption onto biowaste materials of animal and plant origin using 5-level Box-Behnken design: Equilibrium, kinetic, thermodynamic and regeneration studies, J. Rare.Earth. 32 (2014) 745-758. https://doi.org/10.1016/j.jhazmat.2009.09.097

[38] F. Geyikci, E. Kilic, S. Aoruh, S. Elevli, Modelling of lead adsorption from industrial sludge leachate on red mud by using RSM and ANN, Chem. Eng. J. 183(2012) 53-59. https://doi.org/10.1016/j.cej.2011.12.019

[39] G. Chen, J. Chen, C. Srinivasakannan, J.H. Peng, Application of response surface methodology for optimization of the synthesis of synthetic rutile from titania slag, Appl. Surf. Sci. 258 (2012) 3068-3073. https://doi.org/10.1016/j.apsusc.2011.11.039

[40] A. Dehghani, A. Azizi, S.H. Mojtahedzadeh, Kh. Gharibi, Optimizing rougher flotation parameters of the Esfordi phosphate ore, Miner. Process. Extr. Metall. Rev. 33 (2012) 260-268. https://doi.org/10.1080/08827508.2011.584092

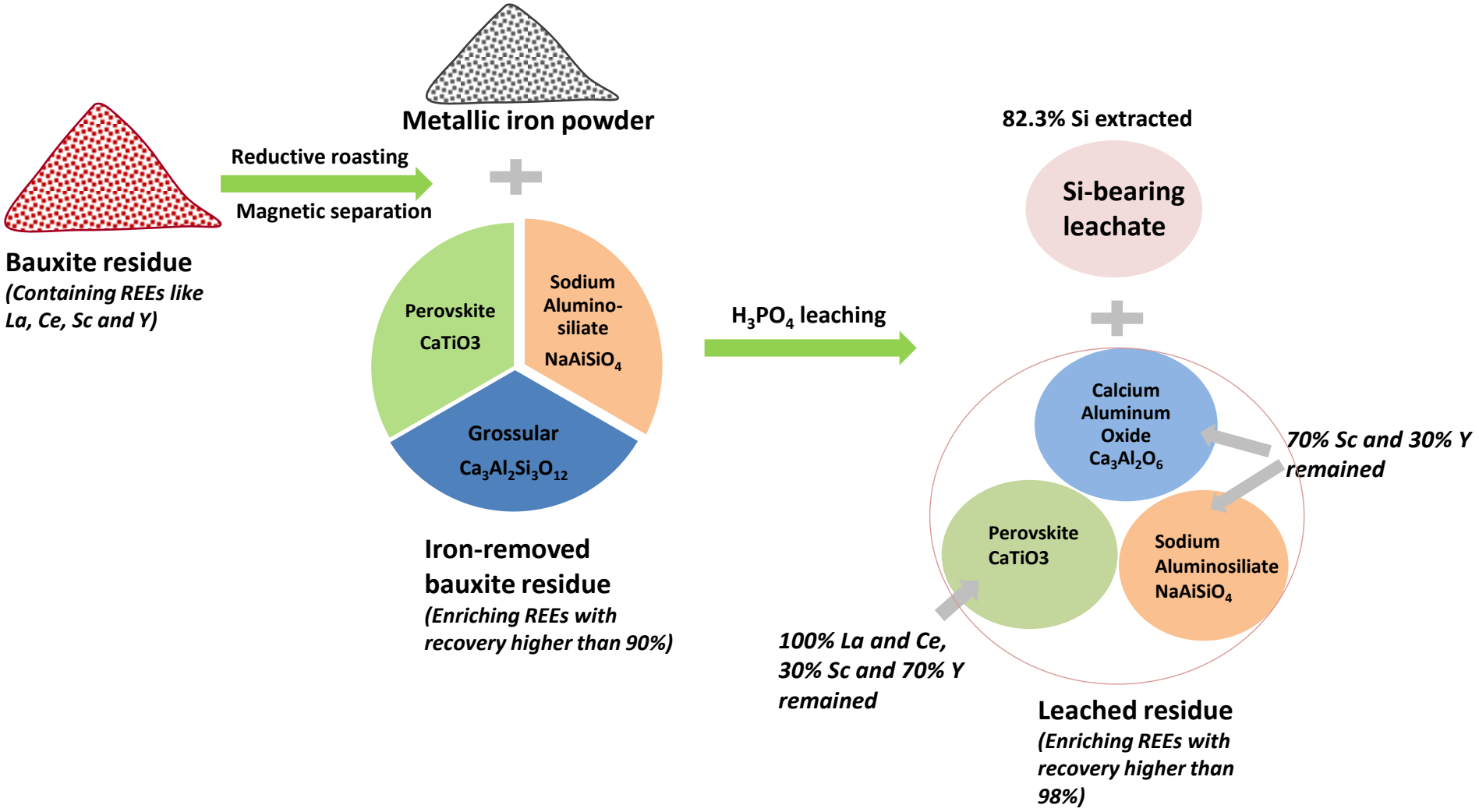
Metallic iron powder
Reductive roasting
Magnetic separation
Bauxite residue
(Containing REEs like La, Ce, Sc and Y)
Perovskite CaTiO3
Sodium Alumino-siliate NaAiSiO4
Grossular Ca3Al2Si3O12
Iron-removed bauxite residue
(Enriching REEs with recovery higher than 90%)
H3PO4 leaching
82.3% Si extracted
Si-bearing leachate
Calcium Aluminum Oxide Ca3Al2O6
70% Sc and 30% Y remained
Perovskite CaTiO3
Sodium Aluminosiliate NaAiSiO4
100% La and Ce, 30% Sc and 70% Y remained
Leached residue
(Enriching REEs with recovery higher than 98%)

Highlights:

(1) Enrichment of multiple REEs (e.g. La_2O_3, Ce_2O_3, Sc_2O_3 and Y_2O_3) with simultaneously removing silica from the iron-removed bauxite residues was achieved by acid leaching with H_3PO_4.

(2) Response surface methodology (RSM) was successfully applied to optimize the leaching process and obtain the optimal leaching conditions.

(3) The enrichment mechanism of various REEs (La_2O_3, Ce_2O_3, Sc_2O_3 and Y_2O_3) during acid leaching was explicated respectively.